The Fermi surface and pseudopotentials of aluminium

The Fermi surface and pseudopotentials of aluminium

A P Horsfield† and N W Ashcroft

Laboratory of Atomic and Solid State Physics, Cornell University, Ithaca, NY 14853-2501, USA

Abstract. The accurately determined energy levels at the W point of the FCC Brillouin zone obtained from low-temperature galvanometric measurements of the Fermi surface of aluminium are used to determine an empirical local pseudopotential and to test the precision of the standard scheme for calculations of band structure. While satisfactory for cohesive and structural properties, the standard scheme appears to reproduce the third-zone Fermi surface dimensions and topology rather poorly. Since there still remains some flexibility in the definition of *ab initio* pseudopotentials, it is suggested that agreement with the major cohesive and structural properties can be maintained, but that with relatively minor adjustment Fermi surface properties can also be reproduced. This notion is illustrated for the empirical local pseudopotential which is applied to the evaluation of the interatomic pair potential (which is found to be in good agreement with other calculated pair potentials) and also to a redetermination of the conductivity of molten aluminium which reveals rather clearly the limitations of the first-order Born approximation.

1. Introduction

Calculation of one-electron properties of condensed matter is an important first step in the reduction of a starting many-body problem. There are several approaches, some of which make use of the density functional theory (DFT) of the electron gas within the Kohn–Sham formulation [1]. Since the exchange–correlation functional is not known exactly, approximations are used, a prominent one being the local density approximation (LDA). To calculate the properties of systems involving more than a very few atoms, it is often necessary to use pseudopotentials to model the interaction between electrons and the ionic cores [2, 3]. These have a number of major advantages over the full coulombic potentials. Specifically, they allow the core electrons to be treated implicitly, thus reducing the number of wavefunctions that have to be handled, and they can be made smooth, so that they can be used subsequently with plane-wave basis sets small enough to be handled without intensive computation. This procedure, when used with *ab initio* pseudopotentials [4–8], will be referred to from here on as the *standard scheme*.

Although the standard scheme is often used with success, there remain questions concerning its accuracy, both for total energies, and for single-particle properties. However, the problem is actually more acute for the single-particle properties. This follows from the observation that in principle DFT can give exact ground-state energies, but may not give correct quasi-particle energies (when used within the Kohn–Sham formulation), such as are found from Fermi surface measurements [9–13]. It is thus of some interest to investigate the errors in the single-particle energies that result from the standard scheme. Note that

† Present address: School of Chemical Engineering, Olin Hall, Cornell University, Ithaca, NY 14853, USA.

only errors produced by the total set of approximations (such as the difference between measured and calculated band structure) will be considered. The individual contributions can only be separated out using a more detailed approach than that presented here.

In this paper the single-particle energy levels near the Fermi energy of aluminium are taken as an example to be investigated. The method used is as follows. First, the energy levels close to the Fermi surface obtained from experiment are determined (this has, in fact, already been carried out [14]). Second, an empirical local pseudopotential is found which, when used with a large plane-wave basis set that leads to completely converged results, accurately reproduces the measured Fermi surface structure. The point is simply to demonstrate that a simple single-particle Hamiltonian reproducing the single-particle levels in crystalline aluminium reliably exists; it does not say that it is unique. Third, the energy levels near the Fermi surface are then calculated using the standard scheme (with the pseudopotentials of Hamann [8]), and these are also compared with the known experimental results. It is found that the results are in poor agreement with experiment, which suggests that pseudopotentials *might* still be improved if experimental information about the Fermi surface were included in the process of constructing them, a point of view that was taken in the early development of pseudopotentials. As is well known, there is some flexibility in the construction of these quantities, and the refinements being proposed are to be carried out within this variability; the overall success of the current schemes is therefore not compromised.

Finally, the empirical pseudopotential is used to calculate two properties of liquid aluminium (an interatomic pair potential, and the electrical conductivity) using simple theories. The interatomic potential is found to agree well with values previously calculated by other authors, and is a further confirmation of the accuracy of the fitted pseudopotential. The electrical conductivity, determined by a Born approximation (the Ziman theory), is found to agree *poorly* with experiment, which confirms that the simple scattering theory is inadequate for the problem.

2. Experimental results

The Fermi surface of aluminium (as well as of many other simple metals) has been measured with great accuracy. In particular there are quite precisely determined cross sections in the third zone whose areas are less than $10^{-3}\pi k_f^2$. Since the Fermi surface for a particular band (or zone) is simply that set of points in the first Brillouin zone, translated from other zones if needed, at which the single-electron levels in that band (or zone) possess the Fermi energy, the existence of these precise dimensions places considerable constraints on the band structure *near* the Fermi energy.

The de Haas–van Alphen measurements of the Fermi surface of aluminium have already been analysed in detail [14] and the levels at the W point $(k = (2\pi/a)(1, \frac{1}{2}, 0))$ are known very precisely. The analysis was carried out within the framework of the empirical pseudopotential method with folding back of the full (infinite by infinite) secular equation, as described in the appendix. Within this approach the band structure near the W point of the first irreducible zone can be modelled using a 4×4 folded secular equation:

$$\begin{vmatrix} T_0(k, \varepsilon) & V_{111} & V_{111} & V_{200} \\ V_{111} & T_1(k, \varepsilon) & V_{200} & V_{111} \\ V_{111} & V_{200} & T_2(k, \varepsilon) & V_{111} \\ V_{200} & V_{111} & V_{111} & T_3(k, \varepsilon) \end{vmatrix} = 0 \qquad (1)$$

where

$$T_0(k, \varepsilon) = \hbar^2 k^2 / 2m - \varepsilon$$

$$T_1(k, \varepsilon) = (\hbar^2/2m)k - (2\pi/a)(1, 1, 1)^2 - \varepsilon$$

$$T_2(k, \varepsilon) = (\hbar^2/2m)k - (2\pi/a)(1, 1, -1)^2 - \varepsilon \qquad (2)$$

$$T_3(k, \varepsilon) = (\hbar^2/2m)k - (2\pi/a)(2, 0, 0)^2 - \varepsilon$$

provided k is restricted to the irreducible zone (see figure 1). Note that these diagonal terms implicitly include other terms from the folding down of an infinite-order secular equation. However, it is also assumed that the terms from folding can still be well modelled by a local potential, also yielding a term V_{000} to be added to the kinetic energy which has the same value for each diagonal term. It contributes only a constant offset to the band structure, and therefore can be set to zero. In equation (1) V_{111} and V_{200} are proportional to the Fourier transform of the effective electron–ion pseudopotentials evaluated at $G = (2\pi/a)(1, 1, 1)$ and $G = (2\pi/a)(2, 0, 0)$ respectively; they include folding corrections as discussed in the appendix.
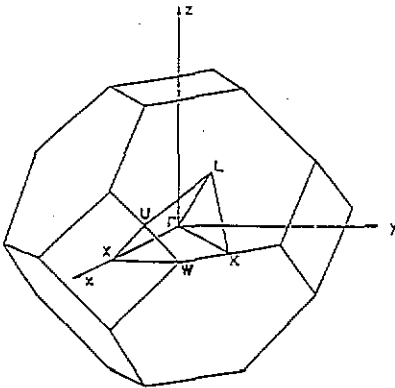

Figure 1. First Brillouin zone of the FCC structure showing the principal points of high symmetry defining the irreducible zone.

In the analysis of reference [14], V_{111} and V_{200} were treated as free parameters, and were determined by direct fitting to the measured Fermi surface. Fitting these parameters to the experimentally determined third-zone Fermi surface sections gives (with $m^*/m = 1$):

$$|V_{111}| = 0.244 \text{ eV} \qquad (3a)$$

and

$$V_{200} = 0.765 \text{ eV}. \qquad (3b)$$

(From the pressure dependence of the optical properties of aluminium, the sign of V_{111} was subsequently fixed as positive [15].) Using these the energies of the first four levels at the W point of the first Brillouin zone, are easily evaluated using

$$W_1 = \varepsilon_W + V_{200} + 2|V_{111}|$$

$$W_2' = \varepsilon_W + V_{200} - 2|V_{111}| \qquad (4)$$

$$W_3 = \varepsilon_W - V_{200} \qquad \text{(doubly degenerate)}$$

where (with $V_{000} = 0$ as described above) $\varepsilon_W = \hbar^2 k_W^2/2m$. From equation (4), the levels near W consistent with the experimentally determined Fermi surface can therefore be summarized by the statements

$$W_1 - W_3 = 2.02 \text{ eV} \qquad W_2' - W_3 = 1.04 \text{ eV}. \tag{5}$$

It is to these two quantities, experimentally fixed, that the empirical pseudopotential is fitted and to which the results of *ab initio* pseudopotential calculations will be primarily compared.

3. An empirical pseudopotential

A local empirical pseudopotential is now determined which, when combined with linear screening, will give accurate band structures using the connectivity of the Fermi surface as a criterion, and especially the small but critical third-zone dimensions. To illustrate the general point being made, the *simplest* possible model incorporating core cancellation is used, namely the empty core pseudopotential defined by

$$V_{ec}(r) = \begin{cases} -Ze^2/r & r > r_c \\ 0 & r < r_c \end{cases} \tag{6}$$

which contains one free parameter (r_c). The value of this effective core radius is chosen such that this form can be used to reproduce the empirically determined energy levels at W (two numbers). Though this choice is suggested by the fact that the core in aluminium is particularly compact and tightly bound, it is important to emphasize that the procedures discussed next can be applied to more general choices of pseudopotential.

The Fourier transform of this pseudopotential (equation (6)) appears in the Hamiltonian matrix, and with linear screening included, the corresponding form factor is

$$V(q) = -(4\pi Ze^2/\Omega q^2) \cos(qr_c)/\varepsilon(q). \tag{7}$$

The screening function used in what follows is that of Hubbard [16], and is given by

$$\varepsilon(q) = 1 + \Pi(q)/[1 - g(q)\Pi(q)]$$

with

$$\Pi = (1/\pi k_f a_0) f(x)/x^2$$

and

$$f(x) = \tfrac{1}{2} + (1 - x^2/4x) \ln |(1+x)/(1-x)| \tag{8}$$

where $x = q/(2k_f)$, and the local field correction is $g = 1/(2 + 1/\alpha x^2)$ with $\alpha = 1 + 0.158/(\pi k_f a_0)$ which is chosen to satisfy the compressibility sum rule on $\varepsilon(q)$. Note that the assumption that many-electron effects can be incorporated within a *linear screening* approximation is a possible source of error in making a later detailed comparison with *ab initio* potentials.

The best value of r_c is found in the following straightforward manner. A value of r_c is declared good to the extent that the eigenvalues of the Hamiltonian constructed with the

potential of equation (7) and which are characterized by the wavevector k_W agree with the experimentally determined eigenvalues given in equation (5). Initial upper and lower bounds on the best value of r_c are found using a basis set (20 Ryd cut-off energy) that is *not* large enough to lead to *complete* convergence of the eigenvalues with respect to basis set size, but which is large enough to provide reliable *bounds*. The range of r_c between the bounds is subsequently decreased while using a much larger basis set (80 Ryd cut-off energy), which does lead to eigenvalues converged with respect to basis set size. The resulting value of r_c for aluminium is 0.709 Å. The form factor resulting from this procedure is plotted in figure 2; it leads to levels with energies of

$$W_1 - W_3 = 2.01 \text{ eV} \qquad W_2' - W_3 = 1.04 \text{ eV} \tag{9}$$

which are seen to be in excellent agreement with the experimental results, given that there is but a single free parameter. Note that a large number of plane waves is needed on account of the long range of the pseudopotential used. Figure 3 shows the convergence of the three energy levels as a function of plane-wave cut-off energy.
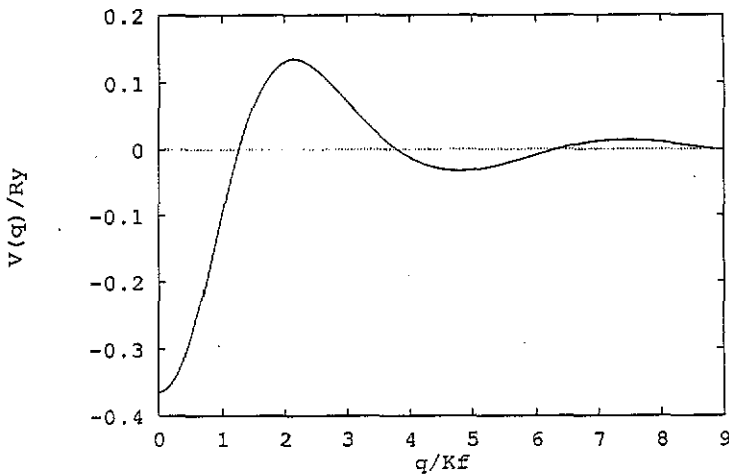

Figure 2. The fitted pseudopotential presented in reciprocal space.

Agreement for the three principal levels at W does not constitute a particularly stringent test by itself; accordingly the bands along a number of symmetry directions were also determined, and the results for *these* are shown in figure 4. They agree well with other calculated band structures (see, for example, [17]). It should be pointed out that because of its simplicity, the present pseudopotential is not expected to be transferable (there is no reason to believe that it would, for instance, give the correct energy levels for an *isolated* atom). However, for the system to which it was fitted, it clearly contains the physically relevant information needed to describe the single-particle energy levels.

There may, of course, be a small possible source of error in the calculated core radius resulting from the use of *linear* screening (as opposed to full non-linear self-consistency) in this simple model. To estimate this, consider the following argument. Imagine that an aluminium ion is embedded in a uniform electron gas, and the electron–ion interaction is described by a pseudopotential. The Kohn–Sham eigenfunctions for the electrons can be
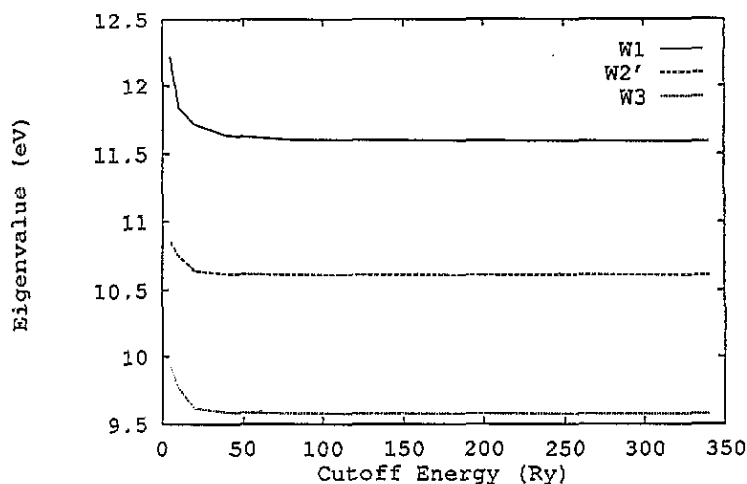
Figure 3. The convergence test for the bands produced using the empty core potential with core radius of 0.7095 Å. The test was done for the four levels used for the comparisons we have been making.
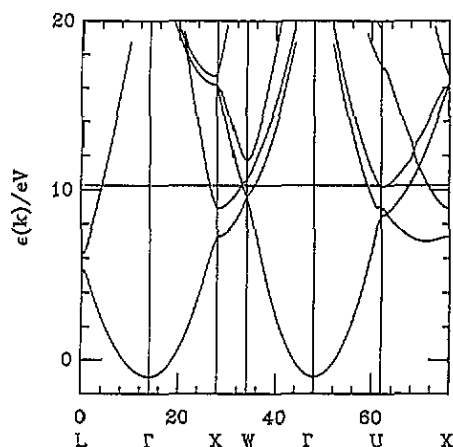

Figure 4. Band structure of aluminium produced using the best fit empty core potential.

calculated, using perturbation theory, to first order in the total Kohn–Sham potential (which includes the pseudopotential, a Hartree term, and an exchange–correlation term). From these eigenfunctions the perturbed electron density can also be calculated, and from this, the requisite Kohn–Sham potential. This leads to a linear self-consistent problem for the Kohn–Sham potential, the solution to which is the linearly screened potential. The total band structure energy (correct to first order in the perturbing potential) can then be calculated. The entire process can also be continued to second order in the perturbing potential. It is possible to separate the errors in the band structure energy into two components: the error in the Hamiltonian (on account of the error in the density used to generate the Kohn–Sham potential), and the error in the eigenfunctions (on account of the truncated perturbation expansion). It is reasonable to suppose that the two sources lead to errors that may be comparable in magnitude since the error in the density exists solely because of errors in the eigenfunctions. That is, the error in the band structure energy on account of the error

in the screening of the potential ought to be of the same order of magnitude as the error in the energy on account of the errors in the eigenfunctions. The latter have been investigated for the phonon spectrum of aluminium [18], and are found to be of the order of a few per cent. This implies an error of corresponding magnitude in the eigenvalues. From this it can be concluded that ignoring screening beyond linear order leads to errors in the eigenvalues of the order of a few per cent. Small as this error may be, it is enough to give the wrong Fermi surface. Thus the choice of r_c must implicitly include corrections for the non-linear screening terms (it is the *screened* pseudopotential that is reliable, and not the bare one). However, it should be stressed that the change in the core radius, if full self-consistency were used, would certainly be small. (In the fitting process a change in r_c was found to lead to a change in $W_1 - W_3$ that corresponds to the same percentage change in the two quantities.)

For the purpose of comparison, it is interesting to note that some values of r_c for the empty core pseudopotential have been determined for aluminium by other authors using quite different methods. A value of r_c that purports to give the correct zero-pressure volume is 0.304 Å [19]; a value obtained from resistivity calculations [20] is $r_c = 0.590$ Å. There is apparently a wide variation in r_c, the value clearly depending on the physical quantity from which the core radius is determined, and the sensitivity of that property to it. However, since the band structure is fundamental (in the one-electron picture) the value of 0.709 Å would seem to be preferred.

4. Results from the standard scheme

The energy levels at the W point of the first Brillouin zone can also be calculated using the *ab initio* pseudopotential of Hamann [8], but using the method developed by Teter and co-workers [21]. For this calculation, plane waves up to an energy of 32.0 Ryd are used, and the calculations are carried out within the local approximation of DFT. A large cell (32 atoms) is taken, with one special k point selected for evaluating the density. The choice of special point $k = (2\pi/a)(\frac{1}{4}, \frac{1}{4}, \frac{1}{4})$ proved to be adequate, as the cell is large (it is equvalent to using the Γ point with a cell containing 256 atoms). Particular care is taken to treat the degeneracies at the Fermi level correctly.

The levels of interest at the W point are then found in this procedure to be

$$W_1 - W_3 = 1.76 \text{ eV} \qquad (10a)$$

and

$$W_2' - W_3 = 1.05 \text{ eV}. \qquad (10b)$$

When compared with experiment, the errors in these levels are seen to be about 1% for $W_2' - W_3$ but 8% for $W_1 - W_3$. The important point is that even a small shift in the energy of the bands in the third zone can actually cause very significant changes in the size of the cross section of the Fermi surface, simply because it is already so small (in [14] it is pointed out that an error of just 0.4% in the Fermi energy can lead to a factor of two in the areas of the small waist-like sections of the third-zone Fermi surface near W). In the present case, the levels at W (see equations (10)) lead to a connectivity of the third-zone Fermi surface which is completely different from the measured topology [14].

It is difficult to decide which approximation will be improved if a correction is now made to a pseudopotential by the *direct incorporation* of experimental data since the

sources of possible error are not easily separable. Equally, it is difficult to say how the pseudopotentials should be modified in a way that leaves essentially intact their more desirable features. However, it seems appropriate to focus on one aspect of constructing *ab initio* pseudopotentials, since it corresponds so closely to the fitting method used here for the demonstration case of an empirical pseudopotential. This is the somewhat arbitrary choice of the radius that separates the core region (which is smoothed in the creation of the pseudopotential) from the rest of space. This radius defines an effective atomic length scale, and perhaps ought not to be treated so arbitrarily (see [22] for an argument supporting a less arbitrary core radius). The Fermi surface has been used to fix this length scale in the example given above, and it is possible that this may be an acceptable procedure to fix the core radius, even for pseudopotentials that have far more physical content than that of equation (6). In regard to this, it should be noted again that within small variations of such length scales, many *ab initio* pseudopotentials give quite acceptable values for structure and cohesive energies.

It is certainly reasonable to ask [23] whether fitting the pseudopotential to measured band structure data, while improving the band structure, might not in general lead to a possible deterioration in other quantities (notably total energy). As already noted, the proposed adjustments are to be carried out within a range of insensitivity for structure and cohesion. But it is also appropriate to observe that the LDA to DFT, so successful in wide band systems, is still an approximation and there is no guarantee, even in principle, that it will reproduce the correct Fermi surface. The states near the Fermi surface are, however, important in transport and in some instances in electron order, such as pairing. Yet these states do not constitute a large fraction of the totality of occupied states, for which the LDA is apparently doing well. Accordingly, it would not be expected that the procedures suggested here will be inimical to existing pseudopotentials.

5. Further applications

Since the single-particle Hamiltonian provides a fundamental, though approximate, description of a system, it is possible to use it to evaluate a number of properties. These properties can in turn be used to check the accuracy of the Hamiltonian by comparing the calculated properties either with experiment or with other calculations. Thus, as a first application, the ionic pair potential for aluminium is computed using the fitted screened pseudopotential simply as a check on the pseudopotential; it is found to give results in good agreement with those obtained by other authors. The electrical conductivity is then evaluated using the standard weak-scattering approximation as a way of testing this approximation. Rather poor agreement with experiment is found, indicating that the weak-scattering approximation is inadequate, but not, now, the input information to the calculation itself.

The state-dependent ionic pair potential is determined within linear response theory; this is straightforward provided that the electron–ion interaction is known. Thus following [3]

$$\Phi(r, r_s) = \frac{(Ze)^2}{r} \left\{ 1 - \frac{2}{\pi} \int_0^\infty \frac{dq}{q} \sin(qr) \left(\frac{v_{ps}(q)}{Z v_C(q)} \right)^2 \left(1 - \frac{1}{\varepsilon(q, r_s)} \right) \right\} \quad (11)$$

where $v_{ps}(q, r_c)$ is the empty core pseudopotential forced, as noted, to fit (care being taken to ensure that eigenvalues are converged with respect to basis set size) to the correct band
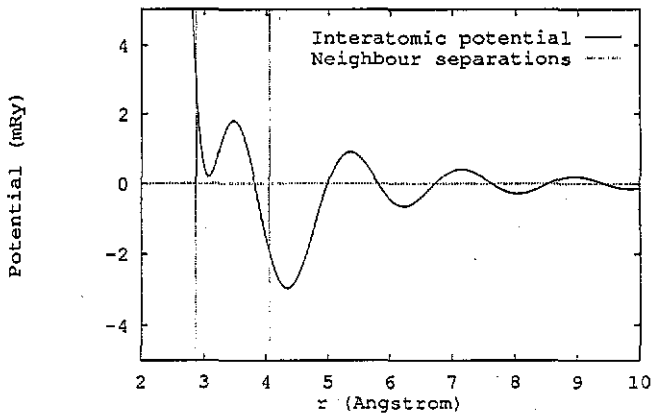
Figure 5. The ion–ion pair potential for aluminium. The two vertical dotted lines correspond to the first- and second-nearest-neighbour separations.

structure, and $v_C(q)$ is the Coulomb potential. We have used the dielectric function of equation (8); the resulting pair potential is plotted in figure 5.

Recently other determinations of this pair potential have been carried out using both the empty core model, and optimized pseudopotentials [24]. They agree well with the potential shown in figure 5. Important features include the following: a repulsive edge at about 3 Å and the lowest minimum at 4.4 Å. There is also a small minimum in the core region which agrees with the non-relativistic core orbital result of [24], but which stands in contrast to the empty core potential result given in that paper. It is worth noting that the location of this minimum is close to the nearest-neighbour separation for aluminium and the deepest minimum is near the second-nearest-neighbour separation.

The resistivity can also be recalculated using the theory of Ziman (see, for example, [25]), from the expression

$$\rho = \left(\frac{\hbar a_0}{e^2}\right)\left(\frac{4\pi Z}{(k_f a_0)^3}\right)\int_0^1 \frac{dy}{y} S(2k_f y)\left(\frac{\cos(2k_f r_c y)}{\varepsilon(2k_f y)}\right)^2 \tag{12}$$

where $S(k)$ is the static structure factor for the liquid phase and $(\hbar a_0/e^2)$ has the numerical value of 21.7 $\mu\Omega$ cm. The pair potential given above is seen to have a very abrupt and steeply repulsive core which, following [25], motivates the use of a hard-sphere structure factor given by

$$S(k) = 1/[1 - nc(k\sigma)] \tag{13}$$

where n is the density of ions, and the Ornstein–Zernike direct correlation function c is given within the Percus–Yevick approximation [26] for the hard-sphere approximation to the pair potential. It is defined by

$$c(k\sigma) = -4\pi\sigma^3 \int_0^1 ds\, s^2 \frac{\sin(sk\sigma)}{sk\sigma}(\alpha + \beta s + \gamma s^3) \tag{14}$$

where

$$\eta = (\pi/6)n\sigma^3 \qquad \alpha = (1 + 2\eta)^2/(1 - \eta)^4$$
$$\beta = -6\eta(1 + \eta/2)^2/(1 - \eta)^4 \qquad \gamma = \tfrac{1}{2}\eta(1 + 2\eta)^2/(1 - \eta)^4. \tag{15}$$

In equations (15) η is the packing fraction and σ is the hard core radius (this has a value of 2.43 Å). We take η to be 0.45 (the value that most classical fluids have at their solidification point) and σ is then given by

$$\sigma = (6\eta/\pi n)^{1/3}. \tag{16}$$

The dielectric function defined in equation (8) is also used in equation (12). The resistivity is calculated and found to be 78 $\mu\Omega$ cm, whereas experiment [25] gives 24.2 $\mu\Omega$ cm. This is quite a significant discrepancy. We know now, by construction, that the electron–ion interaction is reliable (the pseudoptential has been *forced* to give good band structure results). We also know that the Percus–Yevick hard-sphere structure factor gives quite an accurate representation of the static structure factor of liquid aluminium. Accordingly the result indicates a limitation in the weak-scattering transport theory. The point of primary concern is the use of the first-order Born approximation which effectively asserts that an electron has lost all knowledge of one scattering event before it suffers another. But the mean free path is actually of the order of 16 Å which is only a few atomic diameters. Thus we may conclude that the scattering events interfere, leading to a change in the total scattering, and hence a change in the resistivity. (See, for instance, [20, 25, 27] for earlier discussions of the validity of the first-order Born approximation in the calculation of resistivity, given at a time when pseudopotentials were somewhat less reliable than they are now.)

6. Summary

The accurately determined energy levels at the W point of the FCC Brillouin zone obtained from de Haas–van Alphen measurements of the Fermi surface of aluminium are used in two ways. First, an empirical local pseudopotential with one free parameter (r_c) is directly determined by these energy levels. Second, they are used to test the precision of the standard scheme for calculations of band structure (involving a combination of the LDA for the exchange–correlation function within the Kohn–Sham formulation of DFT, with *ab initio* pseudopotentials for the electron–ion interaction). It is found that the standard scheme appears to reproduce the third-zone Fermi surface dimensions rather poorly, but at present it is not possible to say how much of the error is to be ascribed to the pseudopotential, how much to LDA, and how much to DFT. In spite of this, it is proposed that pseudopotentials can be constructed which accurately reproduce one-particle structure near the Fermi energy. An example of such a construct is applied to the evaluation of the ionic pair potential of molten aluminium (which is found to be in good agreement with the pair potentials calculated by Hafner and Jank [24]). It is also used to determine the electrical conductivity of molten aluminium, and is found to give poor agreement with experiment (which reveals somewhat more clearly the limitations of the first-order Born approximation).

Appendix. Folding down of the secular equation

From the Kohn–Sham equations we know that the Schrödinger-type equation includes a Hamiltonian that is dependent on the electron density of the system for which the calculation is being performed. Now suppose this density were known (which in general it is not, and has to be found through imposition of a self-consistency procedure). It is then possible to solve for the eigenvalues and eigenvectors of the Hamiltonian in the following way: take a basis of plane waves, and find the matrix elements of the Hamiltonian. Because of the translational symmetry of the system, only matrix elements of the form $H_{GG'} = \langle k + G | H | k + G' \rangle$ are non-vanishing. Here k is a vector from the first Brillouin zone for the crystal lattice, and G and G' are reciprocal lattice vectors. These matrix elements are then used in the solution of the following matrix equation

$$\sum_{G'} H_{GG'} \Psi_{G'} = \varepsilon \Psi_G. \tag{A1}$$

This equation can be represented in block structure by the diagram shown in figure A1. Here, the Hamiltonian matrix has been formally partitioned into four parts; **A** and **C** are square submatrices, and **B** and **B**† are (in general) rectangular. The corresponding partition of the eigenvector is U and V. The purpose of introducing the block structure is that the matrix equation $H\psi = \varepsilon\psi$ can be rewritten as

$$\mathbf{A}U + \mathbf{B}V = \varepsilon U \qquad \mathbf{B}^\dagger U + \mathbf{C}V = \varepsilon V. \tag{A2}$$

In turn this can be rearranged to give

$$(\mathbf{A} - \mathbf{B}(\mathbf{C} - \varepsilon\mathbf{I})^{-1}\mathbf{B}^\dagger)U = \varepsilon U. \tag{A3}$$

(Note that alternative derivations can be found in [28].) The significance of this equation is that we began with a very large secular equation and have formally reduced it to a smaller one that yields the same eigenvalues and even part of the same eigenvectors. However, the new matrix is now dependent on energy, and if the potential had originally been local, the effective potential in the reduced matrix is now non-local. To see this last point, let us look at the structure of the reduced matrix $\tilde{\mathbf{H}}$, namely

$$\tilde{H}_{GG'} = A_{GG'} - \sum_{G_+ G'_+} B_{GG_+}(C - \varepsilon I)^{-1}_{G_+ G'_+} B^\dagger_{G'_+ G}$$

$$= H_{GG'} - \sum_{G_+ G'_+} H_{GG_+}(H - \varepsilon I)^{-1}_{G_+ G'_+} H_{G'_+ G} \tag{A4}$$

where the subscript $+$ indicates that the reciprocal lattice vector appears in the submatrix **C** and the absence of the subscript means it appears in the submatrix **A**. We imagine that the eigenvalues to be evaluated are quite different from the diagonal terms of submatrix **C**. Thus the terms along the diagonal of $\mathbf{C} - \varepsilon\mathbf{I}$ are non-vanishing. If the off-diagonal terms are negligible by comparison with the diagonal terms, then the inverse of $\mathbf{C} - \varepsilon\mathbf{I}$ can be given approximately by the diagonal matrix with the reciprocal of the diagonal elements of $\mathbf{C} - \varepsilon\mathbf{I}$ down its diagonal. This then gives us the following approximation

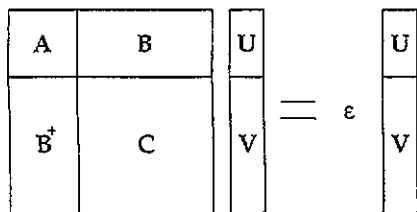$$\tilde{H}_{GG'} \simeq H_{GG'} - \sum_{G_+} \frac{H_{GG_+} H_{G_+ G'}}{H_{G_+ G_+} - \varepsilon}. \tag{A5}$$

Figure A1. Block structure diagram representation of the matrix equation.

We can now see that if the potential in H depended on G and G' only as $G - G'$ (that is, if the potential were local), then the corresponding terms in the reduced matrix will depend on G and G' in a much more complex manner (in fact the equivalent potential is non-local).

   In a particular form of the empirical pseudopotential method, a relatively small matrix $\tilde{H}$ is assumed, the off-diagonal matrix elements of which are treated as free parameters. It is usual to treat these elements as though they were derived from a local potential, and hence their dependence is only on the difference of wave vectors. The values of these matrix elements are then determined by requiring that the band structure produced by these matrix elements agree with some experimentally provided data. These matrix elements can only be used to produce accurate results in the matrix in which they appeared for the fitting. If they need to be used in a matrix of different size, then the process of folding down the matrix has to be reversed to regain the original $H_{GG'}$ before being refolded to obtain the new matrix.

References

[1] Jones R O and Gunnarsson O 1989 *Rev. Mod. Phys.* **61** 689
[2] Heine V 1970 *Solid State Physics* vol 24 (New York: Academic) p 1
[3] Harrison W 1966 *Pseudopotentials in the Theory of Metals* (New York: Benjamin)
[4] Hamann D R, Schlüter M and Chiang C 1979 *Phys. Rev. Lett.* **43** 1494
[5] Kerker G P 1980 *J. Phys. C: Solid State Phys.* **13** L189
[6] Kleinman L and Bylander D 1982 *Phys. Rev. Lett.* **48** 1425
[7] Bachelet G B, Hamann D R and Schlüter M 1982 *Phys. Rev.* B **26** 4199
[8] Hamann D R 1989 *Phys. Rev.* B **40** 2980
[9] Schönhammer K and Gunnarsson O 1988 *Phys. Rev.* B **37** 3128
[10] Mearns D 1988 *Phys. Rev.* B **38** 5906
[11] March N H 1988 *Phys. Rev.* B **38** 10067
[12] Godby R W and Needs R J 1989 *Phys. Rev. Lett.* **62** 1169
[13] Mearns D and Kohn W 1989 *Phys. Rev.* B **39** 10669
[14] Ashcroft N W 1963 *Phil. Mag* **8** 2055
[15] Dandrea R G and Ashcroft N W 1985 *Phys. Rev.* B **32** 6936
[16] Hubbard J 1957 *Proc. R. Soc.* A **243** 336
[17] Moruzzi V L, Janak J F and Williams A R 1978 *Calculated Electronic Properties of Metals* (New York: Pergamon) p 52
[18] Bertoni C M, Bortolani V, Calandra C and Nizzoli F 1974 *J. Phys. F: Met. Phys.* **4** 19
[19] McLaren R E and Sholl C A 1974 *J. Phys. F: Met. Phys.* **4** 2172
[20] Ashcroft N W and Langreth D C 1967 *Phys. Rev.* **159** 500
[21] Teter M, Payne M and Allan D 1989 *Phys. Rev.* B **40** 12255
[22] Goedecker S and Maschke K 1992 *Phys. Rev.* A **45** 88
[23] Teter M 1993 private communication
[24] Hafner J and Jank W 1990 *Phys. Rev.* B **42** 11532
[25] Ashcroft N W and Lekner J 1966 *Phys. Rev.* **145** 83
[26] Hansen J P and McDonald I R 1976 *Theory of Simple Liquids* (London: Academic)
[27] Ashcroft N W and Lawrence W E 1968 *Phys. Rev.* **175** 938
[28] Cohen M L and Heine V 1970 *Solid State Physics* vol 24 (New York: Academic) p 78